Journal of Inorganic Biochemistry 201 (2019) 110833

Contents lists available at ScienceDirect

Journal of Inorganic Biochemistry

journal homepage: www.elsevier.com/locate/jinorgbio

Kinetic analysis of a globin-coupled diguanylate cyclase, YddV: Effects of heme iron redox state, axial ligands, and heme distal mutations on catalysis

Alzbeta Lengalova[1], Veronika Fojtikova-Proskova[1], Jakub Vavra, Václav Martínek, Martin Stranava, Toru Shimizu, Marketa Martinkova*

Department of Biochemistry, Faculty of Science, Charles University, Hlavova (Albertov) 2030/8, Prague 2, Czech Republic

ARTICLE INFO

Keywords:
Heme-based oxygen sensor
Intramolecular catalytic regulation
Signal transduction
Diguanylate cyclase
Globin-coupled oxygen sensor

ABSTRACT

Heme-based oxygen sensors allow bacteria to regulate their activity based on local oxygen levels. YddV, a globin-coupled oxygen sensor with diguanylate cyclase activity from *Escherichia coli*, regulates cyclic-di-GMP synthesis based on oxygen availability. Stable and active samples of the full-length YddV protein were prepared by attaching it to maltose binding protein (MBP). To better understand the full-length protein's structure, the interactions between its domains were examined by performing a kinetic analysis. The diguanylate cyclase reaction catalyzed by YddV-MBP exhibited Michaelis-Menten kinetics. Its pH optimum was 8.5–9.0, and catalysis required either Mg^{2+} or Mn^{2+}; other divalent metal ions gave no activity. The most active form of YddV-MBP had a 5-coordinate Fe(III) heme complex; its kinetic parameters were K_m^{GTP} 84 ± 21 μM and k_{cat} 1.2 min^{-1}. YddV-MBP with heme Fe(II), heme Fe(II)-O_2, and heme Fe(II)-CO complexes had k_{cat} values of 0.3 min^{-1}, 0.95 min^{-1}, and 0.3 min^{-1}, respectively, suggesting that catalysis is regulated by the heme iron's redox state and axial ligand binding. The k_{cat} values for heme Fe(III) complexes of L65G, L65Q, and Y43A YddV-MBP mutants bearing heme distal amino acid replacements were 0.15 min^{-1}, 0.26 min^{-1} and 0.54 min^{-1}, respectively, implying that heme distal residues play key regulatory roles by mediating signal transduction between the sensing and functional domains. Ultracentrifugation and size exclusion chromatography experiments showed that YddV-MBP is primarily dimeric in solution, with a sedimentation coefficient around 8. The inactive heme-free H93A mutant is primarily octameric, suggesting that catalytically active dimer formation requires heme binding.

1. Introduction

Heme-based oxygen sensor proteins give many bacteria unique ways to continuously monitor the composition of their surroundings and regulate intracellular processes to adapt to changing conditions. These proteins have at least two domains: an N-terminal sensing domain and a C-terminal functional domain [1,2]. The heme iron complex is located in the sensing domain and is the oxygen sensing site. Signals generated by the heme's interactions with molecular oxygen are transduced from the sensing domain to the functional domain, causing structural changes in the functional domain that enhance or suppress the protein's catalytic activity, switching it on or off as appropriate [1–3]. A detailed kinetic analysis of heme-based oxygen sensors with different heme iron redox and/or coordination states could shed more light on the molecular mechanism of signal transduction, but few such analyses have been reported.

In general, the sensing domains of heme-based oxygen sensor proteins can adopt diverse conformations and the functional domains can exhibit various catalytic activities [1]. This work focuses on YddV (or *Ec*DosC), a globin-coupled diguanylate cyclase sensor from *E. coli* [4–6]. Globin-coupled oxygen sensors with diguanylate cyclase activity have also been identified in *Pectobacterium carotovorum* (*Pcc*GCS) [7], *Bordetella pertussis* (*Bpe*GReg) [7–11], *Desulfotalea psychrophia* (HemDGC) [12], *Azotobacter vinelandii* (*Av*Greg) [13], and *Shewanella putrefaciens* (*Sp*DosD) [14]. Another protein of this class with putative diguanylate cyclase activity has been found in *Geobacter sulfurreducens* (*Gs*GCS), but its activity has yet to be assessed [15].

Cyclic-di-guanosine-5′-monophosphate (*c*-di-GMP) is an important bacterial second messenger that regulates many key physiological functions including cell motility, differentiation, development, virulence, biofilm formation, cell−cell communication, and environmental persistence [16–18]. Two heme-based oxygen sensors play central roles in *c*-di-GMP signaling cascades in *E. coli*. As noted above, YddV consists of an N-terminal heme-bound oxygen sensing domain with a globin fold

* Corresponding author.
E-mail address: marketa.martinkova@natur.cuni.cz (M. Martinkova).
[1] Both authors contributed equally to this work.

https://doi.org/10.1016/j.jinorgbio.2019.110833
Received 12 June 2019; Received in revised form 3 September 2019; Accepted 5 September 2019
Available online 06 September 2019

and a C-terminal functional domain that catalyzes the formation of *c*-di-GMP from guanosine-5′-triphosphate (GTP). YddV acts in tandem with another heme-based oxygen sensor phosphodiesterase, *Ec*DOS (or *Ec*-DosP), which has an N-terminal heme-bound oxygen sensing domain with a PAS fold (named for the proteins Per - Drosophila period clock protein, Arnt - vertebrate aryl hydrocarbon receptor nuclear translocator, and Sim -Drosophila single-minded protein) and a C-terminal functional domain that catalyzes the conversion of *c*-di-GMP to linear di-GMP [4,19,20]. The phosphodiesterase activity of *Ec*DOS is substantially enhanced by O_2 binding to the heme Fe(II) complex in the sensing domain. It was found that YddV and *Ec*DOS associate to form a functional complex and are translated from a polycistronic operon [21]. Accordingly, the two proteins were co-purified. Their interaction is probably based on hydrophobic forces [4].

The structure and function of the isolated YddV heme-binding domain have been studied extensively [6,22–26]. However, because of the difficulty of preparing a catalytically active version of the full-length YddV protein, only preliminary kinetic analyses of the full-length protein have been reported. These studies revealed that the Fe(III) form of YddV is the most active, while the Fe(II)-O_2 and Fe(II)-CO forms are less active [4–6]. It was also suggested that the Fe(II) form of YddV was significantly less active than other forms [5,6]. However, these studies only analyzed the catalytic activity of the full-length protein in terms of the initial rate of product formation (in micromoles of *c*-di-GMP per micromole of YddV per minute) [4–6]. One of these investigations also indirectly examined the diguanylate cyclase activity of YddV in the presence of the coupled enzyme *Ec*DOS [4].

Here we report the first successful preparation of stable and active full-length YddV, which was achieved by attaching it to maltose binding protein (MBP). To better understand the structure of the full-length protein, the interactions between its sensing and functional domains were examined by performing a detailed kinetic analysis based on its K_m, V_{max} and k_{cat} values. The effects of the heme iron redox state and/or ligand coordination on its catalytic activity were investigated, along with the dependence of the enzyme's kinetic parameters on amino acid residues located on the heme distal side of the Fe(III) complex. The effects of divalent metal cations other than Mg^{2+} on catalysis were also studied. We analyze the interactions between the sensing and functional domains of YddV in terms of changes in the kinetic parameters of its diguanylate cyclase activity under diverse conditions. Specifically, we studied the impact of changes in the heme-containing sensing domain on the diguanylate cyclase activity of the YddV functional domain. Clarifying the relationship between signal transduction, protein conformation, and the functional state of the sensor protein should help explain the molecular mechanism of its sensing activity.

2. Experimental procedures

2.1. Materials

Ampicillin was obtained from P-lab (Prague, Czech Republic). Isopropyl β-D-thiogalactopyranoside, hemin, sodium dithionite, Na_2S, *c*-di-GMP, tris(hydroxymethyl)aminomethane (Tris) and acrylamide were obtained from Sigma-Aldrich (St. Louis, MO, USA) and GTP from GE Healthcare. Water, doubly distilled over quartz, was purified using a Milli-Q Plus system (EMD Millipore, Billerica, MA, USA). All glassware used for sample preparation was conditioned in advance by standing for 24 h in 10% HCl suprapur (Merck, Darmstadt, Germany). All chemicals used were of the highest purity grade available from commercial sources and used without further purification.

2.2. Overexpression and purification of the wild type (WT) and mutant proteins

Nine YddV-MBP protein expression vectors were constructed: pMAL-c5e/WT, R365A, Y43A, Y43F, L65G, L65M, L65Q, L65T and H98A. The previously reported pET21c(+)/YddV plasmid [5] was digested with *Nde*I and *Xho*I, and subcloned into the pMAL-c5e vector (New England Biolabs, USA), leading to the introduction of an MBP protein tag at the N-terminus of the desired protein. The following oligonucleotides were designed to extract the inserts of previously reported YddV mutants (L65 and Y43) from the corresponding pET28a/YddV mutant vectors [5]. Nucleotides for *Nde*I and *Xho*I restriction sites were inserted into the oligonucleotide sequences.

Forward: 5′-AGATACATATGGAGATGTATTTTAAAAGAATG-3′ and reverse: 5′-AGATACTCGAGCTAAAGACTGGCTTTCCAG-3′.

To obtain the YddV-MBP H98A plasmid, the pMAL-c5e/YddV WT plasmid was mutated using the QuikChange II Site-Directed Mutagenesis Kit (Agilent). The following oligonucleotides were used for polymerase chain reaction:

Forward: 5′-CATACCGTCGCGGAAGTGGCTGCCCGCATAGGAATTCC-3′

Reverse: 5′-GGAATTCCTATGCGGGCAGCCACTTCCGCGACGGTATG-3′.

To obtain the gene encoding the YddV-MBP R365A mutant, gene splicing overlap extension polymerase chain reaction was performed using the following oligonucleotides:

Forward pMAL: 5′-CTCGGGGATGACGATG-3′

Reverse pMAL: 5′-CTCTCCTGAGTAGGACAAATC-3′

Forward R365A: 5′-TTATGACAACGTCGCCAGTAGTG-3′

Reverse R365A: 5′-CACTACTGGCGACGTTGTCATAA-3′

Full-length wild-type and mutant variants of YddV-MBP were expressed in *E. coli* BL21(DE3) (Novagen) harboring the pMAL-c5e expression vector. Briefly, *E. coli* BL21(DE3) was transformed with the required plasmid, plated on Luria-Bertani (LB) agar containing 100 μg/ml ampicillin, and incubated at 37 °C overnight. On the following day, a single colony was inoculated in LB containing 100 μg/ml ampicillin and shaken overnight at 200 rpm and 37 °C. The culture medium was added to Terrific Broth medium (1:1000 dilution) containing the above antibiotics and shaken at 120 rpm and 37 °C for 4 h. Subsequently, the medium was cooled to 15 °C and protein expression was induced by adding 0.1 M isopropyl β-D-thiogalactopyranoside, followed by further shaking for 20 h. *E. coli* cells were harvested by centrifugation for 10 min at 6750 *g* and 4 °C, frozen in liquid nitrogen, and stored at −80 °C until purification. *E. coli* cells frozen at −80 °C were suspended in buffer A (50 mM Tris-HCl, pH 8.0, 150 mM NaCl), 1 mM phenylmethanesulfonyl fluoride, 1 mM ethylenediaminetetraacetic acid, and 0.2 mg/ml lysozyme. The solution was sonicated, centrifuged at 100,000*g* for 30 min and incubated for 20 min with hemin (300 μM) in dimethyl sulfoxide solution. Supernatant fractions were applied to an amylase column (Qiagen, Hilden, Germany) pre-equilibrated with buffer A. Subsequently, the column was washed with buffer A and YddV-MBP fractions were eluted with buffer A containing 10 mM maltose. Protein fractions were pooled and applied to a Superdex 200 10/300 GL column (GE Healthcare, UK) equilibrated with 20 mM Tris-HCl pH 8.0 buffer containing 150 mM NaCl. The desired eluates (identified by monitoring at 280 nm) were collected and concentrated with Amicon® Ultra Centrifugal Filters (Millipore, Billerica, MA, USA). Finally, the purified proteins were quickly frozen in liquid nitrogen and stored at −80 °C until use. All proteins were > 95% homogenous as confirmed by SDS-PAGE (sodium dodecyl sulfate polyacrylamide gel electrophoresis). Protein concentrations were determined using the bicinchoninic acid assay with bovine serum albumin as a standard (Sunrise Absorbance Reader, TECAN).

Expression and purification procedures for *Ec*DOS are described in an earlier report [27]. The protein was > 95% homogenous as confirmed by SDS-PAGE. Protein and heme concentrations were determined using the bicinchoninic acid assay with bovine serum albumin as a standard (Sunrise Absorbance Reader, TECAN) and the pyridine hemochromogen assay, respectively.

2.3. Optical absorption spectroscopy

Optical absorption spectral data were obtained at 24 °C using a Cary 60 UV–Vis spectrophotometer (Agilent Technologies, CA, USA). To ensure that the solution was maintained at an appropriate temperature, the reaction mixture was incubated for 5 min prior to spectroscopic measurement.

2.4. Kinetic analysis of the diguanylate cyclase reaction

The diguanylate cyclase activity of YddV-MBP was assayed under various conditions. Unless stated otherwise, the enzymatic reaction was performed at 24 °C, in 50 μl reaction mixtures containing 10 μM YddV-MBP, 50 mM KCl, 5 mM $MgCl_2$, and 50 mM Tris buffer (pH 8.0). The reaction mixture was pre-incubated for 5 min and the reaction was initiated by adding 1 mM GTP (dissolved in Tris buffer, pH 8.0). The incubation time was usually 2.5 min. The reaction was stopped by incubation at 100 °C for 3 min. Each incubation was performed at least in triplicate. The samples were analyzed by HPLC (high-performance liquid chromatography) using Buffer A (0.1 M KH_2PO_4, 4 mM tetrabutyl ammonium hydrogen sulfate, pH 6.0) and Buffer B (75% Buffer A, 25% methanol) at a flow rate of 0.7 ml/min. Elution was performed using 60% A/ 40% B for the first 15 min then 100% B for 6 min before returning to 60% A/40% B. The absorbance of GTP and c-di GMP was monitored at 254 nm as reported previously [19].

The effect of pH on the diguanylate cyclase activity of YddV-MBP was tested in reaction mixtures containing various buffers. Reactions at pH 5.5, 6.0, 6.5 and 7.0 were performed using 100 mM phosphate buffer with an appropriate ratio of Na_2HPO_4 and NaH_2PO_4. Incubations at pH 7.5, 8.0, 8.5, and 9.0 were performed in 100 mM Tris buffer (Tris-HCl), and incubations at pH 9.5, 10.0 and 10.5 were performed using 100 mM glycine (glycine-NaOH) buffer.

The effects of divalent metal ions on YddV-MBP diguanylate cyclase activity were investigated using reaction mixtures containing solutions of metal salts other than $MgCl_2$. Specifically, 5 mM $MgCl_2$ was replaced with 5 mM $MnCl_2$, 5 mM $CaCl_2$, 5 mM $CoCl_2$, 5 mM $NiCl_2$, 5 mM $ZnSO_4$, or 5 mM $CdCl_2$ as appropriate. To assess the enzyme's activity in the absence of divalent metal cations, reactions were performed with no added metal salt. Kinetic constants were determined by fitting the kinetics using the tight-binding (Morrison) equation [28].

The time course of the diguanylate cyclase reaction catalyzed by WT YddV-MBP was assayed at 24 °C in a reaction mixture containing 10 μM WT YddV-MBP, 50 mM Tris-HCl (pH 8.0), 50 mM KCl, and 5 mM $MgCl_2$. The reaction mixture was preincubated for 5 min, and then the reaction was initiated by adding 1 mM GTP at 24 °C. The state of the reaction was determined at 0, 0.5, 1, 2, 3, 5, 15, 30, 45, and 60 min after initiation.

The kinetic parameters of the diguanylate cyclase activity of YddV-MBP were investigated using 50 μl reaction mixtures containing 10 μM YddV-MBP, 0–1000 μM GTP (0, 10, 25, 50, 100, 300, 500, 750, or 1000 μM dissolved in Tris buffer, pH 8.0), 50 mM Tris-HCl (pH 8.0), 50 mM KCl, and 5 mM $MgCl_2$. The reaction was started by adding GTP. On the basis of the previously determined (see the preceding paragraph) time course for the diguanylate cyclase reaction catalyzed by WT YddV-MBP, the amount of reaction product formed per minute over the first 3 min of the reaction was taken as the initial velocity of the enzymatic reaction (Fig. S1). Therefore, the reaction mixtures used to determine kinetic parameters were incubated at 24 °C for 2.5 min; the reaction during this period was assumed to proceed under initial velocity conditions because of the reaction's linearity over the first 3 min. The reaction was stopped by incubation at 100 °C for 3 min. The YddV-MBP diguanylate cyclase reaction is a condensation process (two molecules of the substrate, GTP, are combined to form the product, *c*-di-GMP). Kinetic constants were determined by nonlinear least-squares regression based on the Michaelis − Menten equation. At least three replicate experiments were performed for each set of reaction conditions. Kinetic parameters were determined by fitting based on individual measurements and then averaged and grand standard deviations were calculated from the fit error and discrepancies between individual measurements.

The effects of the heme iron and its redox and coordination state on the Michaelis − Menten kinetics of the diguanylate cyclase reaction were investigated by varying the configuration of the sensing domain heme of YddV-MBP. After purification, the heme iron of the native YddV-MBP protein was in the Fe(III) state. Heme Fe(II) species were prepared by placing a 20 μM solution of the Fe(III) protein in a quartz cuvette and reducing it using 10 mM sodium dithionite in an anaerobic box. Fe(II)-CO complexes were then prepared by gently bubbling gaseous carbon monoxide (Linde, Wiesbaden, Germany) through the cuvette for 5 min. No spectral changes indicative of heme oxidation over time were detected during this process. Sodium dithionite was removed from the preparations containing the Fe(II) and Fe(II)-CO complexes using Sephadex G-25 in PD-10 desalting columns (GE Healthcare), although separate experiments demonstrated that the presence of sodium dithionite did not affect the measured kinetic parameters. The Fe(II)-O_2 complex was prepared by removing sodium dithionite using Sephadex G-25 in PD-10 desalting columns (GE Healthcare) and exposing the Fe (II) species to air for 10 min. After the kinetic experiments, we characterized the samples by UV–Vis spectroscopy to verify that the heme iron species remained in the Fe(II)-O_2 form. These studies revealed no evidence of heme iron autoxidation over the course of the experiment in the case of WT YddV-MBP. The Fe(III)-CN^- and Fe(III)-imidazole forms of YddV-MBP were produced by mixing a 20 μM solution of the native YddV-MBP protein in its Fe(III) form with 0.1 M KCN and 0.1 M imidazole, respectively. The KCN was used in 100 mM Tris buffer (pH 8.0), and the solution's pH was monitored. Heme-free experiments were performed using the H98A YddV-MBP mutant instead of the WT protein.

The effects of key amino acids on the heme distal side of the sensing domain on the Michaelis − Menten kinetics of the diguanylate cyclase reaction catalyzed by YddV-MBP were investigated by testing mutant proteins in which selected amino acids of WT YddV-MBP were replaced, namely Y43A, Y43F, L65G, L65 M, L65Q, and L65 T. The heme iron was in the oxidation state (forming the Fe(III) complex) in all these proteins. At least three replicate experiments were performed for each mutant. As before, kinetic parameters for each mutant were determined by fitting based on individual measurements then averaging, and grand standard deviations were calculated from the fit error and discrepancies between individual measurements.

To test for possible feedback inhibition of diguanylate cyclase activity by the reaction product, *c*-di-GMP, the activity of YddV-MBP R365A mutant was investigated under the conditions used to study WT YddV-MBP, with the mutant replacing the WT protein. The heme iron center in this protein was in the oxidized state (forming the Fe(III) complex).

2.5. Analytical ultracentrifugation

Sedimentation velocity experiments were performed using a ProteomLab XL-I (Beckman Coulter, Brea, CA) analytical ultracentrifuge at loading concentrations of 1–10 μM YddV-MBP WT, 20 °C, and a rotor speed of 36,000 rpm. Samples were dialyzed against a buffer containing 20 mM Tris-HCl (pH 8.0) containing 150 mM NaCl prior to analysis. All data were collected using interference optics (used for weight average sedimentation coefficient calculations) and absorbance optics at 390 nm (selective for hemoproteins). Sedimentation velocity data were analyzed using a continuous sedimentation coefficient distribution model, c(s). The resulting apparent sedimentation coefficients were used to compute sedimentation coefficients in water at 20 °C (s20,w).

2.6. Size exclusion chromatography

The oligomerization states of YddV-MBP WT and its mutants were determined by size exclusion chromatography using a Superdex 200 Increase 10/300 GL column (GE Healthcare). The mobile phase consisted of 20 mM Tris-HCl (pH 8.0), and 150 mM NaCl. The flow rate was 0.75 ml/min and the injection volume was 100 µl. Eluted proteins were detected by their absorbance at 280 nm. The globular proteins thyroglobulin (669 kDa), apoferritin (481 kDa), aldolase (158 kDa), bovine serum albumin (66 kDa) and ovalbumin (43 kDa) were used as molecular weight standards, and were analyzed on a Superdex 200 Increase 10/300 GL column (GE Healthcare). The calibration data are shown in Fig. S2C and D. The theoretical molecular weights (calculated molecular weights based on amino acid sequences) of YddV-MBP in its monomeric, dimeric, and tetrameric forms are 96 kDa, 192 kDa and 384 kDa, respectively. The calibration data indicate that the column should adequately separate these forms under the conditions applied. The ratios of the content of each oligomeric form were calculated from the peak areas observed in the size exclusion chromatograms.

Samples for analysis were prepared as follows. YddV-MBP WT and mutants in their Fe(III) and other forms (see below) were dissolved in 50 mM Tris-HCl, pH 8.0, 50 mM KCl and 5 mM $MgCl_2$ to a final concentration of 10 µM and incubated at 24 °C for 30 min prior to analysis. The native proteins were in their Fe(III) forms, as they were when isolated. The Fe(II)-O_2 complexes were prepared by incubating proteins with sodium dithionite (0.1 M), removing excess sodium dithionite using a Sephadex G-25 in PD-10 Desalting Column (GE Healthcare), and exposing the resulting Fe(II) species to air for 10 min. The Fe(III)-CN^- and Fe(III)-imidazole forms of YddV-MBP were produced by mixing a 10 µM solution of the native YddV-MBP protein with 10 mM KCN (10 min incubation) and 10 mM imidazole (1 min incubation), respectively. The KCN was used in 50 mM Tris buffer (pH 8.0), and the solution's pH was monitored. After the size exclusion chromatography experiments, we characterized the samples by UV − Vis spectroscopy to verify that the heme iron species remained in the desired form. The samples of YddV-MBP in the presence of *c*-di-GMP were prepared by incubating 10 µM protein with 1 mM GTP, 50 mM KCl. and 5 mM $MgCl_2$ to maximize completion of the diguanylate cyclase reaction (or 0.1 mM *c*-di-GMP) for 5 min at 24 °C. In experiments on the effect of *Ec*DOS on the oligomeric state of YddV-MBP, both proteins were mixed together, each at 10 µM, in 20 mM Tris-HCl (pH 8.0) and 150 mM NaCl, and the mixture was incubated for 30 min at 24 °C prior to analysis.

3. Results

The active full-length YddV protein has proven to be difficult to purify, resisting several standard methods of protein purification. The most efficient approach was to make a chimeric form of the full-length YddV protein fused with maltose binding protein (MBP) at its *N*-terminus. Removing the MBP from the purified YddV-MBP construct caused the immediate precipitation of the liberated YddV protein. Therefore, all studies presented here were conducted with the full-length YddV construct including the MBP tag (YddV-MBP). The UV–Vis spectral properties of the YddV-MBP construct (Supporting Table S1) are virtually identical to those of the isolated globin domain of YddV (YddV-heme) [5,22]. Based on the positions of the Soret band and other peaks in the visible region, the heme iron complex in purified YddV-MBP is a 5-coordinate high-spin Fe(III) complex.

I. The effect of the heme iron redox state and ligand coordination in the sensing domain on the kinetic parameters of the diguanylate cyclase reaction catalyzed by YddV-MBP

The time course of the reaction catalyzed by YddV-MBP indicated that the concentration of the reaction product (*c*-di-GMP) increased linearly during at least the first 3 min (Fig. S1). The reaction rate did

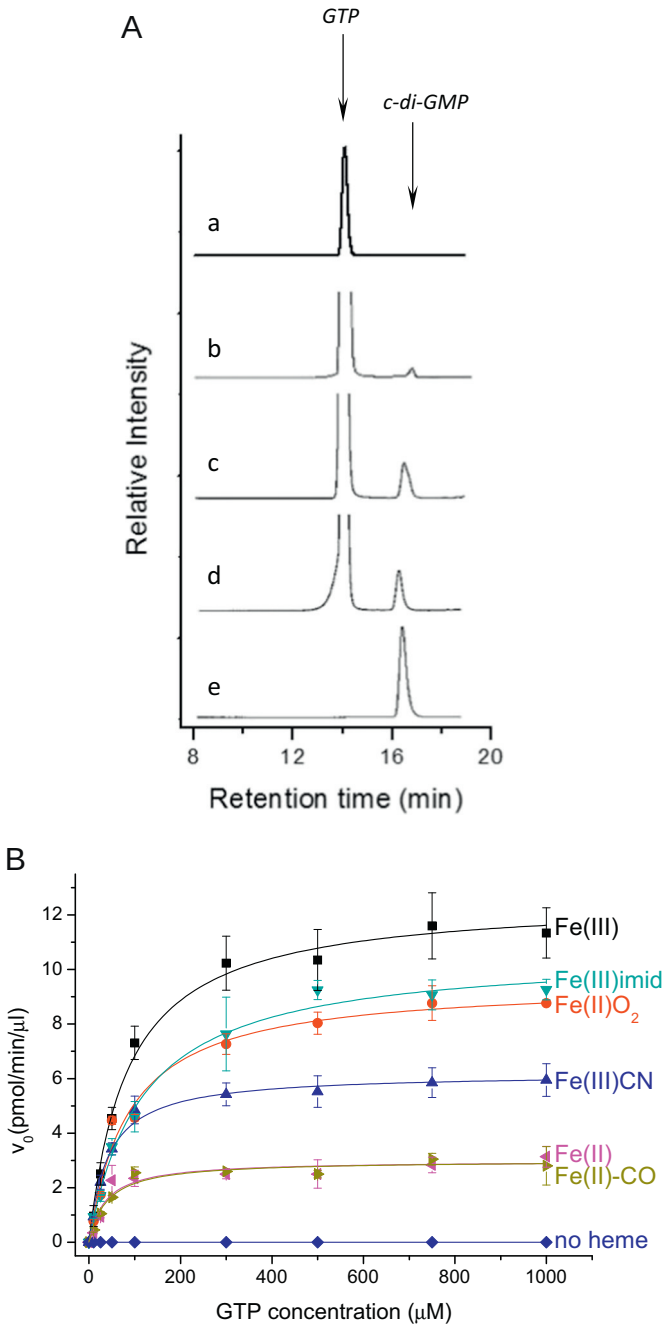

Fig. 1. A HPLC profiles showing the relative abundance of the substrate (GTP) and product (*c*-di-GMP) of the diguanylcyclase reaction catalyzed by YddV-MBP under various conditions. (a): GTP in enzyme-free buffer. (b): GTP after treatment with YddV-MBP in its Fe(II) form. (c): GTP after treatment with YddV-MBP in its Fe(III)-CN form. (d): GTP after treatment with YddV-MBP in its Fe (III) form. (e): *c*-di-GMP in enzyme-free buffer.
B. Effects of the heme iron center's redox state and coordination, and the presence of the heme iron in the sensing domain, on the Michaelis − Menten kinetics of the diguanylate cyclase reaction catalyzed by YddV-MBP. Results for the different forms of YddV-MBP are plotted using the following colors and symbols: Fe(III) (native form; black line and squares), Fe(III)-imidazole (green line and triangles), Fe(II)-O_2 (red line and circles), Fe(III)-CN^- (blue line and triangles), Fe(II)-CO (brown green line and triangles), Fe(II) (pink line and triangles), and heme-free form (H98A; dark blue line and diamonds). In each run, a reaction mixture containing 10 µM of the appropriate YddV-MBP species, 0–1000 µM GTP, 50 mM Tris-HCl (pH 8.0), 50 mM KCl, and 5 mM $MgCl_2$ in a total volume of 100 µl was incubated for 2.5 min (for further details, see Experimental procedures). (For interpretation of the references to color in this figure legend, the reader is referred to the web version of this article.)

Table 1
Effects of the heme iron redox state, heme iron ligand coordination, and the presence of the heme iron in the sensing domain on the kinetic parameters of the diguanylate cyclase reaction catalyzed by YddV-MBP.

Heme iron state in the sensing domain of YddV-MBP	K_m^{GTP} (μM)	V_{max}^{GTP} (pmol *c*-di-GMP·min^{-1}·μl^{-1})	k_{cat} (min^{-1})	k_{cat}/K_m^{GTP} (μM^{-1}·min^{-1})
Fe(III)	84 ± 21	12 ± 1	1.2 ± 0.1	0.014
Fe(III)-CN^-	41 ± 8	6.2 ± 0.5	0.62 ± 0.05	0.015
Fe(III)-imidazole	131 ± 34	12 ± 0.6	1.2 ± 0.06	0.009
Fe(II)-O_2	87 ± 17	9.5 ± 0.5	0.95 ± 0.05	0.011
Fe(II)-CO	39 ± 12	3.0 ± 0.3	0.3 ± 0.03	0.008
Fe(II)	38 ± 19	3.0 ± 0.3	0.3 ± 0.03	0.008
No heme (H98A)		No reaction		

not change appreciably during extended incubations (Fig. S1), suggesting that YddV-MBP is not subject to significant feedback inhibition by the reaction product, *c*-di-GMP. The initial velocities of catalysis were calculated from the slopes of plots of product concentration against time over the first 2.5 min. The reaction kinetics were then analyzed at various GTP concentrations (Fig. 1). Each data set was curve-fitted to the Michaelis-Menten equation using the Hill coefficient (n = 1), revealing that the reactions of all the various YddV-MBP species exhibited Michaelis − Menten kinetics.

To determine whether the heme iron complex in the globin domain is essential for the activity of YddV-MBP, the His98 residue that acts as the proximal axial ligand of the heme Fe(III) complex was replaced with Ala. This led to the formation of heme-free YddV-MBP, as demonstrated by UV–Vis spectroscopy [5]. The heme-free YddV-MBP is inactive, indicating that the heme iron complex is essential for the catalytic activity of YddV-MBP (Fig. 1 and Table 1).

The purified YddV-MBP has a 5-coordinate high-spin Fe(III) complex that is stable under aerobic conditions. This enzyme exhibits high activity, with an apparent Michaelis-Menten constant (K_m^{GTP}) of 84 ± 21 μM, an apparent reaction rate constant or maximal turnover number (k_{cat}) of 1.2 min^{-1}, a catalytic efficiency (k_{cat}/K_m^{GTP}) of 0.014 μM^{-1}·min^{-1} (Table 1), and a V_{max}^{GTP} of 12 pmol *c*-di-GMP·min^{-1}·μl^{-1}. The Fe(II) and Fe(II)-CO species have much lower V_{max}^{GTP} values (0.3 pmol *c*-di-GMP·min^{-1}·μl^{-1}) than the Fe(III) species but their K_m^{GTP} values (38–39 μM) were within ± 50% of that for the Fe (III) species (Table 1, Fig. 1). The heme redox and/or coordination state significantly affected the k_{cat} values. For example, the enzymes with Fe (II) and Fe(II)-CO complexes had a k_{cat} of 0.3 min^{-1}, around 4 times lower than that of the enzyme with the Fe(III) complex (1.2 min^{-1}). Consequently, these enzymes had the lowest k_{cat}/K_m^{GTP} (0.008 μM^{-1}·min^{-1}) values of the studied WT YddV-MBP species (the highest k_{cat}/K_m^{GTP} observed in this work was 0.015 μM^{-1}·min^{-1}). When the enzyme with the Fe(II) complex was exposed to O_2, its catalytic activity increased significantly, suggesting that YddV is an oxygen sensing enzyme (Table 1, Fig. 1). The kinetic parameters of the enzyme with the Fe(II)-O_2 complex closely resemble those of the Fe(III) species.

The K_m^{GTP} (41 μM) and V_{max}^{GTP} (6.2 pmol *c*-di-GMP·min^{-1}·μl^{-1}) of the enzyme with the Fe(III)-CN^- complex were around half those for the Fe(III) species. Conversely, the K_m^{GTP} of the enzyme with the Fe (III)-imidazole complex (131 μM) was almost twice that of the Fe(III) species, although its V_{max}^{GTP} (12 pmol *c*-di-GMP·min^{-1}·μl^{-1}) was similar to that of the Fe(III) species (Table 1, Fig. 1). The k_{cat} (0.62 min^{-1}) of the Fe(III)-CN^- enzyme was half that for the Fe(III) species, but that for the Fe(III)-imidazole enzyme was similar to that for the Fe(III) species. Therefore, the catalytic efficiency (k_{cat}/K_m^{GTP}) (0.015 μM^{-1}·min^{-1}) of the Fe(III)-CN^- species was comparable to that of the Fe(III) species, whereas that (0.009 μM^{-1}·min^{-1}) of the Fe(III)-imidazole species was lower than that of the Fe(III) species. These differences in catalytic efficiency between the Fe(III)-CN^- and Fe(III)-imidazole species are due to their significantly different Michaelis constants (K_m^{GTP}) and k_{cat} values (Table 1, Fig. 1). The protein structural changes at the heme binding site caused by imidazole binding would be larger than those due to cyanide binding. Structural changes in the vicinity of the sensing domain are presumably transduced through the protein's structure to the functional domain, explaining the greater impact of imidazole on the enzyme's K_m^{GTP}.

II. The effect of the Tyr43 and Leu65 residues in the sensing domain on the kinetic parameters of the diguanylate cyclase reaction catalyzed by YddV-MBP

Tyr43 and Leu65 are highly conserved amino acid residues on the heme distal side of the YddV sensing domain. Tyr43 interacts with an oxygen molecule coordinated to the heme Fe(II) complex [5], while Leu65 is critical for restricting the access of water molecules to the heme distal side to avoid rapid YddV autooxidation [22] (Fig. 2A). Mutating these key heme distal amino acids had significant effects on the kinetic parameters of YddV-MBP (Table 2, Fig. 2B). For example, the K_m^{GTP} (22 μM), V_{max}^{GTP} (1.5 pmol *c*-di-GMP ·min^{-1}·μl^{-1}), and k_{cat} (0.15 min^{-1}) of L65G were the lowest of those for any of the YddV variants studied in this work, including the WT. While the K_m^{GTP} (101 μM) of L65Q was higher than those of other variants, its V_{max}^{GTP} (2.6 pmol *c*-di-GMP ·min^{-1}·μl^{-1}) and k_{cat} (0.26 min^{-1}) were the second lowest after those of L65G, giving it the lowest k_{cat}/K_m^{GTP} (0.003 μM^{-1}·min^{-1}) of the proteins studied here. The spectroscopic characteristics of L65G also differed substantially from those of the WT and other Leu65 mutants, indicating differences in structure and the rates of O_2 binding and autooxidation. These results suggest that the water molecule is bound near the heme distal side in both the Fe(III) and Fe(II)-O_2 L65G species [22]. The globin domain structure near the heme prosthetic group of the L65G mutant is probably the most different from the other tested mutants. All of the protein structure changes in the vicinity of the YddV-MBP heme caused by mutations at Leu65 markedly affect the heme Fe(III) enzyme's catalytic kinetics.

The kinetic parameters of the Tyr43 mutants were less striking than those of the Leu65 mutants. The comparatively modest impact of Tyr43 mutations is unsurprising because Tyr43 interacts with the bound O_2 molecule in the Fe(II)-O_2 complex [5]. Therefore, its side chain would be expected to project in a different direction or the residue would be expected to be positioned relatively far from the heme in the Fe(III) form of the enzyme.

III. Effects of other factors (pH, Mg^{2+}, Mn^{2+}, Ca^{2+}, Co^{2+}, Ni^{2+}, Zn^{2+}, and Cd^{2+} ions) on the kinetic parameters of the diguanylate cyclase reaction catalyzed by YddV-MBP

The enzyme was inactive below pH 6.0 and above pH 10.0 (Fig. 3A). Within this range, its activity exhibited an asymmetric bell-shaped dependence upon pH. Its optimal pH was around 8.5–9.00; the rate of catalysis at pH 7.0 was around half that at the optimal pH, while at pH 8.0, it was around 80% of the optimal rate. We conducted our experiments at pH 8.0 because these mildly alkaline conditions are optimal for preserving the conformation and stability of YddV-MBP and

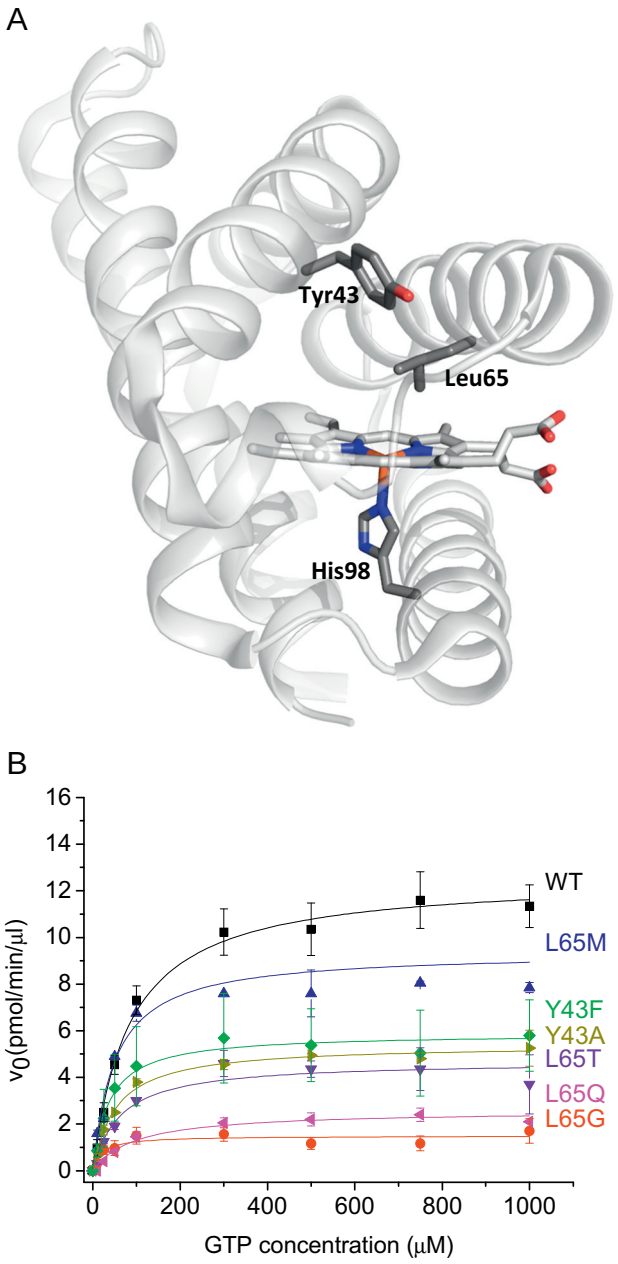

Fig. 2. A. Structure of the YddV sensing domain adopting the globin fold with the heme iron in its Fe(III) form based on PDB coordinates 4ZVA [6]. Heme and sidechains of important residues are shown as sticks.
B. Effects of key amino acids on the heme distal side of the sensing domain on the Michaelis – Menten kinetics of the diguanylate cyclase reaction catalyzed by YddV-MBP. Results for the wild type YddV-MBP are selected mutants plotted using the following colors and symbols: Fe(III) (wild type; black line and squares), L65G (red line and circles), L65M (blue line and triangles), L65T (purple line and triangles), L65Q (pink line and triangles), Y43A (brown line and triangles), and Y43F (green line and diamonds). In each run, a reaction mixture containing 10 µM YddV-MBP WT or mutant, 0–1000 µM GTP, 50 mM Tris-HCl (pH 8.0), 50 mM KCl, and 5 mM $MgCl_2$ in a total volume of 100 µl was incubated for 2.5 min (for further details, see Experimental procedures). (For interpretation of the references to color in this figure legend, the reader is referred to the web version of this article.)

are close to the optimal pH.

We tested the effects of several divalent metal cations (Mg^{2+}, Mn^{2+}, Ca^{2+}, Co^{2+}, Ni^{2+}, Zn^{2+}, and Cd^{2+}) on catalysis under the same conditions (Fig. 3B). No reaction was observed in the absence of divalent metal cations. Of the divalent cations investigated, Mn^{2+} was by far the most effective at stimulating catalysis: the k_{cat}/K_m^{GTP} values in the presence of Mn^{2+} and Mg^{2+} were 0.067 $\mu M^{-1}\cdot min^{-1}$ and 0.016 $\mu M^{-1}\cdot min^{-1}$, respectively. Kinetic constants were determined by fitting the kinetics using the tight-binding (Morrison) equation [28]. The apparent K_m^{GTP} value in the presence of Mn^{2+} (15 ± 4 µM) was approximately 5 times lower than that in the presence of Mg^{2+} (76 ± 5 µM), while the V_{max}^{GTP} (10 ± 0.4 pmol of *c*-di-GMP.min^{-1}.μl^{-1}) and k_{cat} (1.0 min^{-1}) values in the presence of Mn^{2+} were slightly lower than those (12 ± 0.2 pmol of *c*-di-GMP.min^{-1}.μl^{-1} and 1.2 min^{-1}) in the presence of Mg^{2+} (Table 1 and Fig. 3B). Since both Mg^{2+} and Mn^{2+} form metal-GTP complexes, these results suggest that the enzyme's affinity for the Mn^{2+}-GTP complex and the orientation of GTP in its active site differ from those for the Mg^{2+}-GTP complex. Replacing Mg^{2+} with Ca^{2+}, Co^{2+}, Ni^{2+}, Zn^{2+}, or Cd^{2+} completely suppressed the enzyme's activity (Fig. 3B).

Table 2
Effects of key amino acid residues on the heme distal side of the sensing domain on the kinetic parameters of the diguanylate cyclase reaction catalyzed by YddV-MBP.

Mutant of YddV-MBP Fe(III)	K_m^{GTP} (µM)	V_{max}^{GTP} (pmol *c*-di-GMP $\cdot min^{-1}\cdot\mu l^{-1}$)	k_{cat} (min^{-1})	k_{cat}/K_m^{GTP} ($\mu M^{-1}\cdot min^{-1}$)
WT	84 ± 21	12 ± 1	1.2 ± 0.1	0.014
L65G	22 ± 19	1.5 ± 0.3	0.15 ± 0.03	0.007
L65M	42 ± 8	8.5 ± 0.4	0.85 ± 0.04	0.020
L65T	63 ± 25	4.7 ± 0.8	0.47 ± 0.08	0.007
L65Q	101 ± 33	2.6 ± 0.2	0.26 ± 0.02	0.003
Y43A	54 ± 11	5.4 ± 0.3	0.54 ± 0.03	0.010
Y43F	29 ± 10	6.9 ± 0.8	0.69 ± 0.08	0.024

IV. Oligomeric state of YddV-MBP

Because the catalytic activities of other globin-coupled oxygen sensors (*Pcc*GCS and *Bpe*GReg) depend on their oligomerization [7,8], the oligomeric state of YddV-MBP was examined. Ultracentrifugation experiments revealed that WT YddV-MBP predominantly exists as a dimer with a sedimentation coefficient ($s_{20,w}$) of around 8. A tetrameric form with a sedimentation coefficient of around 12 was also present in solution as a minor contributor (Fig. S2A). To study the oligomeric states of YddV-MBP under various conditions, size exclusion chromatography was used as a faster alternative to ultracentrifugation (Fig. S2B). The theoretical molecular weights of YddV-MBP in its monomeric, dimeric, and tetrameric forms are 96 kDa, 192 kDa and 384 kDa, respectively. The chromatographic experiments confirmed that YddV-MBP exists mainly as a dimer, in keeping with the results obtained by ultracentrifigation (Fig. S2A), and indicated that the oligomeric state of YddV-MBP is almost completely independent of the presence or absence of *c*-di-GMP (Fig. S2B). The protein containing the heme iron in its Fe (III) is fully enzymatically active and therefore forms *c*-di-GMP in the presence of GTP (and the other necessary compounds mentioned in the Experimental Procedures). The dimer to tetramer ratios for YddV-MBP in the presence and absence of GTP (and therefore of *c*-di-GMP) were 3.7:1 and 4.3:1, respectively (Fig. S2B).

The effect of the heme iron's oxidation state and ligand coordination on the oligomeric state of YddV-MBP as revealed by size exclusion chromatography is shown in Fig. S3A. Like the Fe(III) form, the Fe(II)-O_2, Fe(III)-CN^-, and Fe(III)-imidazole forms of YddV-MBP exist primarily as dimers, with tetramers being minor components (Fig. S3A). This suggests that changes in the heme iron's oxidation state and ligand coordination have little effect on the protein's oligomerization. Unfortunately, efforts to perform size exclusion chromatography with Fe(II) species under anaerobic conditions were unsuccessful. Importantly, the enzymatically inactive YddV-MBP apoform (H98A) exists predominantly as an octamer (its dimer/tetramer/octamer ratio

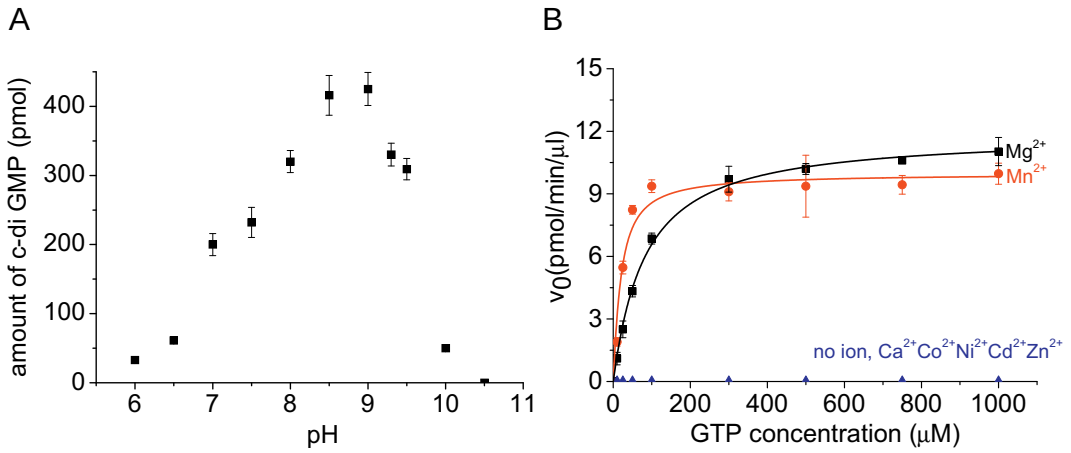

Fig. 3. Effect of pH and divalent metal ions on the diguanylate cyclase reaction catalyzed by WT YddV-MBP [in its Fe(III) form] (A) Effect of pH on the diguanylate cyclase reaction. In each run, a reaction mixture containing 10 µM YddV-MBP, 1 mM GTP, 50 mM KCl, 5 mM $MgCl_2$, and an appropriate pH buffer (100 mM) in a total volume of 100 µl was incubated for 2.5 min (for further details, see Experimental Procedures). (B) Effects of different divalent metal ions on the diguanylate cyclase reaction, plotted using the following colors and symbols: Mg^{2+} (black line and squares; $K_m^{GTP} = 76 \pm 5$ µM and $V_{max}^{GTP} = 12 \pm 0.2$ pmol of *c*-di-GMP.min^{-1}.$µl^{-1}$), Mn^{2+} (red line and circles; $K_m^{GTP} = 15 \pm 4$ µM and $V_{max}^{GTP} = 10 \pm 0.4$ pmol of *c*-di-GMP.min^{-1}.$µl^{-1}$), Ca^{2+}, Co^{2+}, Ni^{2+}, Zn^{2+}, and Cd^{2+}, and no divalent cations (blue line and diamonds). In each run, a reaction mixture containing 10 µM YddV-MBP, 5–1000 µM GTP, 50 mM Tris-HCl (pH 8.0), 50 mM KCl, and 0 or 5 mM $MgCl_2$, 5 mM $MnCl_2$, 5 mM $CaCl_2$, 5 mM $CoCl_2$, 5 mM $NiCl_2$, 5 mM $ZnSO_4$, or 5 mM $CdCl_2$ in a total volume of 100 µl was incubated for 2.5 min (for further details, see Experimental Procedures). (For interpretation of the references to color in this figure legend, the reader is referred to the web version of this article.)

was 1/0/8.4) (Fig. S3A), suggesting that the heme iron complex plays an important role in dimer formation, which may stabilize the enzyme and maximize its catalytic activity.

The effects of key sensing domain amino acids on the oligomeric state of YddV-MBP are shown in Fig. S3B and C. The key amino acids in the sensing domain have stronger effects on the oligomerization of YddV-MBP than the heme iron oxidation and ligand coordination state (Fig. S3B and C). The mutants have a much greater propensity to exist as octamers than the WT protein, for which the abundance of this oligomer was negligible. The relative abundance of the octamer is highest for the Y43F mutant, followed by the L65G mutant (Fig. S3B). It is also interesting that no tetramers were detected in the cases of the L65G, L65Q, and L65 T mutants. The calculated dimer:tetramer:octamer ratios are 4.3:1:~0 for the WT; 3.6:1:1.7 for Y43A; 1.5:1:2.5 for Y43F; 1:~0:1 for L65G; 2.5:~0:1 for L65Q; 1.8:~0:1 for L65T; and 5.2:1:1.2 for L65M. Experiments were also performed using the Fe(III), Fe(II)-O_2, and Fe(III)-CN^- complexes of the Tyr43 (Y43A, Y43F) and Leu65 (L65G, L65M, L65Q, L65T) mutants. However, the results obtained were very similar to those for the Fe(III) forms, so only results for the latter are shown (Fig. S3C). The presence or absence of *c*-di-GMP has no detectable effect on the protein's oligomerization state.

The effect of *Ec*DOS on the oligomerization of YddV was also investigated because it appears that YddV (a *c*-di-GMP synthesizing enzyme) and *Ec*DOS (a *c*-di-GMP degrading enzyme) work together to regulate *c*-di-GMP levels in *E. coli* [4]. However, *Ec*DOS has no detectable effect on the oligomerization state of YddV-MBP when both proteins are present in equimolar quantities (data not shown). Under our experimental conditions, changes in the oligomerization of YddV-MBP would only be observed if the two proteins formed a complex with very high affinity. Our results therefore do not exclude the possibility that *Ec*DOS and YddV interact.

4. Discussion

The molecular mechanism of signal transduction in YddV has remained unclear because of the difficulty of obtaining a catalytically active version of the full-length YddV protein [5,6]. We investigated several approaches to obtain a stable and active form of the full-length YddV protein. The most successful approach involved attaching maltose binding protein (MBP) to full-length YddV at the *N*-terminus. However, it was impossible to remove the MBP tag because the YddV protein precipitated immediately upon doing so. Fortunately, the attachment of MBP to the heme-bound sensing domain has no discernible effect on the UV–Vis spectra of YddV-MBP, which are virtually identical to those of the isolated YddV sensing domain, suggesting that the heme sensing domain of the fusion protein adopts the native structure [5,22] (Supporting Table S1). In addition, the enzyme activities observed in this study for YddV-MBP are significantly higher than those reported previously [4–6]. It thus seems that the MBP tag does not affect the sensing or catalytic activity of YddV, making YddV-MBP a suitable model for studying YddV's kinetics.

Previous studies analyzed the catalytic activity of YddV only in terms of the initial rate of product formation (in micromoles of *c*-di-GMP per micromole of YddV per minute) [4–6]. Those investigations suggested that the Fe(III) form of YddV is more active than the Fe(II)-O_2 and Fe(II)-CO forms [4–6], and that the Fe(II) form is either completely inactive [5] or much less active than the other forms [6]. The initial rates of *c*-di-GMP formation for the Fe(III), Fe(II), Fe(II)-O_2, and Fe(II)-CO species were estimated to be 0.066–0.124 min^{-1}, < 0.001 min^{-1}, 0.022–0.066 min^{-1}, and 0.022 min^{-1}, respectively [5,6]. In this work, we performed detailed kinetic analyses of YddV's catalytic activity and determined the K_m, V_{max} and k_{cat} values of its various forms, allowing us to investigate how changes in the sensing domain affected its kinetics. We also demonstrated that its catalytic activity exhibits Michaelis-Menten kinetics, that the pH optimum for the process is about 8.5–9.0, and that its activity requires the presence of either Mg^{2+} or Mn^{2+}; no diguanyate cyclase activity was observed in the presence of other common divalent metal cations (Ca^{2+}, Co^{2+}, Ni^{2+}, Zn^{2+}, and Cd^{2+}).

In agreement with previous studies, we found that the most active heme iron oxidation and/or coordination form of YddV-MBP is its Fe(III) form. YddV-MBP was isolated in this form under aerobic conditions. However, it may be that the Fe(II) form predominates under anaerobic conditions, and that O_2 binding to this form stimulates catalysis transiently in certain microenvironments. It is possible that YddV acts as both an O_2 sensor and a redox sensor in the cell. In this context, it should be noted that the oxygen-binding affinity of YddV is relatively low (dissociation constant K_d = 15 µM) [22], supporting the possibility

that it may act as a redox sensor. The k_{cat} values of the less active forms of YddV-MBP are around 4 times lower than that of the Fe(III) form, but their catalytic efficiency is only around 2 times lower. The comparatively modest reduction in efficiency is due to a decrease in the K_m^{GTP} value, suggesting that the less active forms have a greater affinity for GTP than the most active form. This may be because of a complex rearrangement of the functional domain associated with the signal transduction process. Interestingly, the less-active Fe(II) form is activated by the binding of O_2, but not by that of CO. It thus seems that the heme distal side of the sensing domain distinguishes between these diatomic molecules. The oxygen sensor *Af*GcHK can also discriminate between these molecules [29], but the oxygen sensor protein *Ec*DOS cannot [19]. The introduction of a sixth axial ligand on the heme iron Fe(III) center also had interesting effects on the enzyme's activity: the small diatomic CN^- ion reduced the K_m^{GTP} value, suggesting an increase in the enzyme's affinity for its substrate (GTP). The difference in affinity between these two forms is comparable to that observed for the Fe(II) and Fe(II)-CO forms. In contrast, the more sterically demanding ligand imidazole caused the K_m^{GTP} value to increase, indicating a reduction in substrate affinity. However, the maximum velocity of the Fe (III)-imidazole form was identical to that of the Fe(III) form. The detailed kinetic analysis thus sheds more light on the changes in the sensing and functional domains (in terms of GTP affinity) caused by the signal transduction process. The importance of these results is amplified by the fact that the full-length protein's low solubility has prevented the acquisition of reliable structural data.

The cyclase activity of the other enzymatically characterized globin-coupled diguanylate cyclases (*Pcc*GCS and *Bpe*GReg) depends on the heme iron's oxidation state and ligand binding to the heme, in keeping with our conclusions regarding YddV [7,8]. Additionally, the K_m^{GTP} values of these sensors in their active and less active forms are comparable to the corresponding values estimated for YddV-MBP: the K_m^{GTP} values for the active Fe(II)-O_2 forms of *Pcc*GCS and *Bpe*GReg were 31 ± 6 μM and 57 ± 8 μM, respectively. The k_{cat} values for *Pcc*GCS Fe(II)-O_2 and *Bpe*GReg were 0.73 min^{-1} and 0.59 min^{-1}, respectively. The less active Fe(II) forms of these enzymes exhibited K_m^{GTP} values of 62 ± 3 μM and 120 ± 11 μM, respectively, and k_{cat} values of 0.29 min^{-1} and 0.18 min^{-1}, respectively [7,8]. Although V_{max}^{GTP} values were not estimated for other globin-coupled diguanylate cyclases, the initial rates reported for these enzymes can be compared to the k_{cat} values presented here. The initial velocities for the active Fe (II)-O_2 form and less active Fe(II) forms of the globin-coupled diguanylate cyclases from *Shewanella putrefaciens* (*Sp*DosD) were 1.68 min^{-1} and 0.52 min^{-1}, respectively; the K_m^{GTP} and V_{max}^{GTP} for this protein were not measured [14]. All these values are similar to those estimated for the active and less active forms of YddV-MBP. However, the initial velocity of the active Fe(II)-O_2 form of another globin-coupled oxygen sensor diguanylate cyclase, HemDGC, is 6.9 min^{-1} – almost an order of magnitude higher than that of similar sensors. Additionally, all other redox and ligand-bound forms of this enzyme exhibited negligible activity [12]. These findings revealed that some organisms with globin-coupled diguanylate cyclases having similar sensing properties [7,8] are probably relatively closely related (*E. coli*, *Bordetella pertussis*, *Pectobacterium carotovorum*), while others are more evolutionarily distant (*Desulfotalea psychrophia)* [12].

Both O_2 binding to the heme within the globin (sensing) domain and *c*-di-GMP binding to a product-binding inhibitory site (I-site) within the cyclase domain control the oligomerization states of *Pcc*GCS and *Bpe*GReg [7,8]. We observed no such oligomerization-dependent differences in activity for YddV-MBP *in vitro*. YddV-MBP exists primarily as a dimer independently of its heme redox state, the heme's ligand coordination, and the presence or absence of the reaction product, *c*-di-GMP. However, mutations of heme distal residues increased the relative abundance of the tetramer and decreased that of the dimer (Figs. S2 and S3). Although globin-coupled diguanylate cyclases from *E. coli, Bordetella pertussis* and *Pectobacterium carotovorum* exhibit some notable similarities [7,8], we showed that there are also significant differences in their behavior.

The functional domain of the YddV-MBP H98A mutant, which lacks a heme in its sensing domain, is catalytically inactive (Table 1 and Fig. 1). Similarly, the activity of a YddV construct without the globin domain was approximately four times lower than that of the Fe(III) form of the full-length protein [6]. These results are consistent with those obtained for a heme-based oxygen sensor phosphodiesterase from *Acetobacter xylinum*, *Ax*PDEA [30], a heme-based oxygen sensor adenylate cyclase from *Leishmania*, HemAC-*Lm* [31], and globin-coupled histidine kinase from *Anaeromyxobacter sp*. Fw109 − 5, *Af*GcHK [29]. The heme-free forms of *Ax*PDEA and HemAc-*Lm* exhibited very low activity. The binding of heme to the sensing domain presumably causes significant and profound structural changes in the active site that enables the efficient activation of these heme-based oxygen sensors. However, the functional effects of heme removal differ from those in the heme-based oxygen sensor phosphodiesterase *Ec*DOS, whose heme-free forms have appreciable catalytic activity. It was suggested that the heme iron complexes of *Ec*DOS may suppress catalysis, and that O_2 binding to the heme iron complex relieves this suppression [20]. Conversely, the YddV-MBP apoform (*i.e.* the H98A mutant) has no heme-binding capacity, exists primarily as an octamer rather than a dimer, and lacks catalytic activity (Table 1, Figs. 1 and S3). This suggests that the dimeric form adopts a fold or conformation that is required for catalysis.

Experiments involving mutating key amino acids in the sensing domain of YddV-MBP yielded remarkable results (Table 2 and Fig. 2B). Leu65 on the heme distal side probably restricts the access of water molecules to the heme iron complex in the WT protein, while the OH side chain of Tyr43 appears to interact directly with O_2 bound to the heme Fe(II) on the heme distal side [22,26]. The activities of Leu65 and Tyr43 mutants seemed to be partially related to the autooxidation rates of the corresponding mutants of the isolated YddV globin domain: mutations that cause high rates of autooxidation in the isolated domain [22] caused low activity in the intact protein, even when only the Fe (III) forms were considered (Supporting Table S2). In addition, the relative abundance of tetramers appeared to be higher for YddV-MBP variants bearing mutations that reduce activity (Table 2 and Fig. S3B and C).

Taking all these results together, we studied the impact of changes in the heme-containing sensing domain on the diguanylate cyclase activity of the YddV functional domain. The results obtained expand our general knowledge of the relationships between signal transduction, protein conformation, and the functional state of YddV, which is important given the lack robust structural data on the full-length protein.

Moreover, we note that the intracellular concentration of GTP in *E. coli* ranges from 0.2 to 1.2 mM depending on the carbon source present in the growth medium [32]. Therefore, the GTP concentration will always significantly exceed the K_m^{GTP} values for the YddV-MBP diguanylate cyclase enzyme reported here. This implies that the rate-limiting step is not substrate recognition (and so K_m^{GTP} is not the most useful kinetic parameter for analyzing trends in YddV's activity) even though the signal transduction process apparently involves some appreciable conformational changes. Instead, the limiting step is probably one of the chemical reactions associated with GTP cyclization. The diguanylate cyclase chemical reaction can be characterized in terms of the V_{max}^{GTP} (or the k_{cat}, which is calculated from V_{max}^{GTP}). Therefore, V_{max}^{GTP} is the most useful kinetic parameter when analyzing the diguanylate cyclase process catalyzed by YddV in the *E. coli* cells.

There are many heme-based oxygen sensors. There are also several different classes of heme domain with different protein folds that bind oxygen and regulate the activity of the catalytic domain. For example, the heme domains of YddV and other globin-coupled oxygen sensors have the globin fold, while those of FixL and *Ec*DOS have the PAS fold, and those of DevS and DevT have the GAF fold (named for the proteins cGMP-specific and -stimulated phosphodiesterase, adenylate cyclase,

and *E. coli* formate hydrogen lyase transcriptional activator) [1–3]. Some of the observed functional differences between the studied proteins may thus be due to differences in protein fold and function.

The diguanylate cyclase enzyme activity of YddV should also be considered in relation to that of the PAS domain-coupled phosphodiesterase *Ec*DOS because these two proteins act together to regulate intracellular *c*-di-GMP levels. The activity of YddV species decreases in the order Fe(III) > Fe(II)-O_2 > > Fe(II)-CO and Fe(II), while that of *Ec*DOS species increases in the order Fe(II)-CO > Fe(II)-O_2 > > > Fe(II) > Fe(III) [19,20]. Because we already know that the substrate concentration in *E. coli* cells substantially exceeds the K_m^{GTP} values for the different YddV-MBP species, the overall rate of the process is determined by V_{max}^{GTP}. While the kinetic parameters of the reaction catalyzed by *Ec*DOS are unknown, it is likely that the concentration of its substrate, *c*-di-GMP, is much lower than that of GTP. Therefore, the rate of the phosphodiesterase process may be governed by the affinity of *c*-di-GMP for individual *Ec*DOS species, unlike in the case of YddV. Moreover, there are probably other factors in the cells that influence the oxygen sensing process and the concentration of *c*-di-GMP. Local milieu- and time-dependent changes/differences in the O_2 concentration in cells will affect the *c*-di-GMP concentration because the O_2 affinities of YddV (K_d: 14 μM) [5] and *Ec*DOS (K_d: 340 μM) [33] differ markedly.

Finally, it should be noted that H_2S is another important signaling gas molecule in bacteria that interacts with the hemes of some heme-based oxygen sensors (including *Ec*DOS, and *Af*GcHK) and affects their catalytic activities [34–37]. We therefore investigated its effect on the UV–Vis spectra and catalytic activities of the heme Fe(III) form of YddV-MBP. Adding H_2S to solutions of this protein caused spectral changes indicative of redox and coordination changes but had no significant effect on its catalytic activity (See Supporting data).

5. Summary

A catalytically active form of the full-length YddV protein was prepared by attaching it to maltose-binding protein (MBP) and subjected to rigorous kinetic analysis. This revealed that:

1. The diguanylate cyclase reaction catalyzed by YddV-MBP exhibits Michaelis-Menten kinetics, has a pH optimum of around 8.5–9.0, and requires the presence of either Mg^{2+} or Mn^{2+}. The most catalytically active form of YddV-MBP was that with a 5-coordinate heme Fe(III) complex; the kinetic parameters determined for this species were K_m^{GTP} 84 ± 21 μM, V_{max}^{GTP} 12 ± 1 pmol of *c*-di-GMP.min^{-1}.μl^{-1}, k_{cat} 1.2 min^{-1}, and k_{cat}/K_m^{GTP} 0.014 μM^{-1}·min^{-1}.

2. The k_{cat} values of YddV-MBP species with heme Fe(II), heme Fe(II)-O_2, and heme Fe(II)-CO complexes were 0.3 min^{-1}, 0.95 min^{-1} and 0.3 min^{-1}, respectively, suggesting that catalysis is regulated by the heme iron center's redox state and axial ligand binding.

3. The k_{cat} values of the heme Fe(III) forms of YddV-MBP variants bearing the L65G, L65Q, and Y43A mutations at heme distal sites were 0.15 min^{-1}, 0.26 min^{-1} and 0.54 min^{-1}, respectively, implying that heme distal amino acid residues play key roles in the catalytic mechanism of YddV because they mediate signal transduction between the sensing and functional domains.

4. Ultracentrifugation and size exclusion chromatography experiments indicated that YddV-MBP predominantly exists as a dimer in solution, with a sedimentation coefficient ($s_{20,w}$) around 8. Conversely, the catalytically inert heme-free mutant H93A was predominantly octameric, suggesting that heme binding is important for formation of the catalytically active dimer.

The results presented here improve our knowledge about the effects of various heme iron redox and axial coordination states on the diguanylate cyclase activity of YddV. Since the heme iron is localized in the protein's sensing domain while the digualylate cyclase activity is localized in its functional domain, we learned more about the relationship between the domains and the signal transduction process. The approach used in this work provided useful insights into the signaling mechanism of YddV, which is particularly important given the lack of structural data on the full-length protein.

Table of abbreviations

*Af*GcHK	a globin-coupled histidine kinase from *Anaeromyxobacter sp.* Fw109 − 5
*Ax*PDEA	a heme-based oxygen sensor phosphodiesterase of *Acetobacter xylinum*
*Bpe*GReg	a globin-coupled oxygen sensor with diguanylate cyclase activity from *Bordetella pertussis*
c-di-GMP	cyclic-di-GMP
*Ec*DOS	a heme-based oxygen sensor phosphodiesterase or *Ec*DosP
E. coli	*Escherichia coli*
Fe(II)	Fe(II)-protoporphyrin IX complex
Fe(III)	Fe(III)-protoporphyrin IX complex, or hemin
GAF	protein domain named after three proteins: cGMP-specific and -stimulated phosphodiesterase, adenylate cyclase, and *E. coli* formate hydrogen lyase transcriptional activator
GMP	guanosine-5′-monophosphate
GTP	guanosine-5′-triphosphate
HemAC-*Lm*	a heme-based oxygen sensor adenylate cyclase of *Leishmania*
HemDGC	a globin-coupled oxygen sensor with diguanylate cyclase activity from *Desulfotalea psychrophia*
HPLC	high-performance liquid chromatography
MBP	maltose binding protein
PAS	protein domain named after three proteins (Per-Arnt-Sim)
*Pcc*GCS	a globin-coupled oxygen sensor with diguanylate cyclase activity from *Pectobacterium carotovorum*
SDS-PAGE	sodium dodecyl sulfate polyacrylamide gel electrophoresis
*Sp*DosD	a globin-coupled oxygen sensor with diguanylate cyclase from *Shewanella putrefaciens*
Tris	tris(hydroxymethyl)aminomethane
WT	wild type
YddV	a globin-coupled oxygen sensor diguanylate cyclase or *Ec*DosC
YddV-heme	an isolated heme-bound globin domain of YddV
YddV-MBP	a full-length YddV protein containing a MBP tag

Acknowledgments

This work was supported in part by Charles University, Czech Republic (SVV260427/2018) and the Grant Agency of Charles University, Czech Republic (grant 704217). CIISB research infrastructure project LM2015043 funded by MEYS CR is gratefully acknowledge for the financial support of the measurements at the CMS.

Appendix A. Supplementary data

Supplementary data to this article can be found online at https://doi.org/10.1016/j.jinorgbio.2019.110833.

References

[1] M. Martínková, K. Kitanishi, T. Shimizu, Heme-based globin-coupled oxygen sensors: linking oxygen binding to functional regulation of diguanylate cyclase, histidine kinase, and methyl-accepting chemotaxis, J. Biol. Chem. 288 (2013) 27702–27711, https://doi.org/10.1074/jbc.R113.473249.

[2] T. Shimizu, D. Huang, F. Yan, M. Stranava, M. Bartosova, V. Fojtíková, M. Martínková, Gaseous O2, NO, and CO in signal transduction: structure and function relationships of heme-based gas sensors and heme-redox sensors, Chem. Rev. 115 (2015) 6491–6533, https://doi.org/10.1021/acs.chemrev.5b00018.

[3] J.A. Walker, S. Rivera, E.E. Weinert, Mechanism and role of globin-coupled sensor signalling, Adv. Microb. Physiol. 71 (2017) 133–169, https://doi.org/10.1016/bs.ampbs.2017.05.003.

[4] J.R. Tuckerman, G. Gonzalez, E.H.S. Sousa, X. Wan, J.A. Saito, M. Alam, M.-

A. Gilles-Gonzalez, An oxygen-sensing diguanylate cyclase and phosphodiesterase couple for c-di-GMP control, Biochemistry 48 (2009) 9764–9774, https://doi.org/10.1021/bi901409g.
[5] K. Kitanishi, K. Kobayashi, Y. Kawamura, I. Ishigami, T. Ogura, K. Nakajima, J. Igarashi, A. Tanaka, T. Shimizu, Important roles of Tyr43 at the putative heme distal side in the oxygen recognition and stability of the Fe(II)-O2 complex of YddV, a globin-coupled heme-based oxygen sensor diguanylate cyclase, Biochemistry 49 (2010) 10381–10393, https://doi.org/10.1021/bi100733q.
[6] M. Tarnawski, T.R.M. Barends, I. Schlichting, Structural analysis of an oxygen-regulated diguanylate cyclase, Acta Crystallogr. D Biol. Crystallogr. 71 (2015) 2158–2177, https://doi.org/10.1107/S139900471501545X.
[7] J.L. Burns, D.D. Deer, E.E. Weinert, Oligomeric state affects oxygen dissociation and diguanylate cyclase activity of globin coupled sensors, Mol. BioSyst. 10 (2014) 2823–2826, https://doi.org/10.1039/c4mb00366g.
[8] J.L. Burns, S. Rivera, D.D. Deer, S.C. Joynt, D. Dvorak, E.E. Weinert, Oxygen and bis (3′,5′)-cyclic dimeric guanosine monophosphate binding control oligomerization state equilibria of diguanylate cyclase-containing globin coupled sensors, Biochemistry 55 (2016) 6642–6651, https://doi.org/10.1021/acs.biochem.6b00526.
[9] X. Wan, J.R. Tuckerman, J.A. Saito, T.A.K. Freitas, J.S. Newhouse, J.R. Denery, M.Y. Galperin, G. Gonzalez, M.-A. Gilles-Gonzalez, M. Alam, Globins synthesize the second messenger bis-(3′-5′)-cyclic diguanosine monophosphate in bacteria, J. Mol. Biol. 388 (2009) 262–270, https://doi.org/10.1016/j.jmb.2009.03.015.
[10] S. Rivera, J.L. Burns, G.E. Vansuch, B. Chica, E.E. Weinert, Globin domain interactions control heme pocket conformation and oligomerization of globin coupled sensors, J. Inorg. Biochem. 164 (2016) 70–76, https://doi.org/10.1016/j.jinorgbio.2016.08.016.
[11] S. Rivera, P.G. Young, E.D. Hoffer, G.E. Vansuch, C.L. Metzler, C.M. Dunham, E.E. Weinert, Structural insights into oxygen-dependent signal transduction within globin coupled sensors, Inorg. Chem. 57 (2018) 14386–14395, https://doi.org/10.1021/acs.inorgchem.8b02584.
[12] H. Sawai, S. Yoshioka, T. Uchida, M. Hyodo, Y. Hayakawa, K. Ishimori, S. Aono, Molecular oxygen regulates the enzymatic activity of a heme-containing diguanylate cyclase (HemDGC) for the synthesis of cyclic di-GMP, Biochim. Biophys. Acta 1804 (2010) 166–172, https://doi.org/10.1016/j.bbapap.2009.09.028.
[13] L. Thijs, E. Vinck, A. Bolli, F. Trandafir, X. Wan, D. Hoogewijs, M. Coletta, A. Fago, R.E. Weber, S. Van Doorslaer, P. Ascenzi, M. Alam, L. Moens, S. Dewilde, Characterization of a globin-coupled oxygen sensor with a gene-regulating function, J. Biol. Chem. 282 (2007) 37325–37340, https://doi.org/10.1074/jbc.M705541200.
[14] C. Wu, Y.-Y. Cheng, H. Yin, X.-N. Song, W.-W. Li, X.-X. Zhou, L.-P. Zhao, L.-J. Tian, J.-C. Han, H.-Q. Yu, Oxygen promotes biofilm formation of Shewanella putrefaciens CN32 through a diguanylate cyclase and an adhesin, Sci. Rep. 3 (2013) 1945, https://doi.org/10.1038/srep01945.
[15] A. Pesce, L. Thijs, M. Nardini, F. Desmet, L. Sisinni, L. Gourlay, A. Bolli, M. Coletta, S. Van Doorslaer, X. Wan, M. Alam, P. Ascenzi, L. Moens, M. Bolognesi, S. Dewilde, HisE11 and HisF8 provide bis-histidyl heme hexa-coordination in the globin domain of Geobacter sulfurreducens globin-coupled sensor, J. Mol. Biol. 386 (2009) 246–260, https://doi.org/10.1016/j.jmb.2008.12.023.
[16] R. Hengge, Principles of c-di-GMP signalling in bacteria, Nat. Rev. Microbiol. 7 (2009) 263–273, https://doi.org/10.1038/nrmicro2109.
[17] T. Schirmer, U. Jenal, Structural and mechanistic determinants of c-di-GMP signalling, Nat. Rev. Microbiol. 7 (2009) 724–735, https://doi.org/10.1038/nrmicro2203.
[18] J.R. Tuckerman, G. Gonzalez, M.-A. Gilles-Gonzalez, Cyclic di-GMP activation of polynucleotide phosphorylase signal-dependent RNA processing, J. Mol. Biol. 407 (2011) 633–639, https://doi.org/10.1016/j.jmb.2011.02.019.
[19] A. Tanaka, H. Takahashi, T. Shimizu, Critical role of the heme axial ligand, Met95, in locking catalysis of the phosphodiesterase from Escherichia coli (Ec DOS) toward cyclic diGMP, J. Biol. Chem. 282 (2007) 21301–21307, https://doi.org/10.1074/jbc.M701920200.
[20] A. Tanaka, T. Shimizu, Ligand binding to the Fe(III)-protoporphyrin IX complex of phosphodiesterase from Escherichia coli (Ec DOS) markedly enhances catalysis of cyclic di-GMP: roles of Met95, Arg97, and Phe113 of the putative heme distal side in catalytic regulation and ligand binding, Biochemistry 47 (2008) 13438–13446, https://doi.org/10.1021/bi8012017.
[21] L. Tagliabue, A. Maciag, D. Antoniani, P. Landini, The yddV-dos operon controls biofilm formation through the regulation of genes encoding curli fibers' subunits in aerobically growing Escherichia coli, FEMS Immunol. Med. Microbiol. 59 (2010) 477–484, https://doi.org/10.1111/j.1574-695X.2010.00702.x.
[22] K. Nakajima, K. Kitanishi, K. Kobayashi, N. Kobayashi, J. Igarashi, T. Shimizu, Leu65 in the heme distal side is critical for the stability of the Fe(II)-O2 complex of YddV, a globin-coupled oxygen sensor diguanylate cyclase, J. Inorg. Biochem. 108 (2012) 163–170, https://doi.org/10.1016/j.jinorgbio.2011.09.019.
[23] J.-C. Lambry, M. Stranava, L. Lobato, M. Martinkova, T. Shimizu, U. Liebl, M.H. Vos, Ultrafast spectroscopy evidence for picosecond ligand exchange at the binding site of a heme protein: heme-based sensor YddV, J. Phys. Chem. Lett. 7 (2016) 69–74, https://doi.org/10.1021/acs.jpclett.5b02517.
[24] A. Pavlou, M. Martínková, T. Shimizu, K. Kitanishi, M. Stranava, A. Loullis, E. Pinakoulaki, Probing the ligand recognition and discrimination environment of the globin-coupled oxygen sensor protein YddV by FTIR and time-resolved step-scan FTIR spectroscopy, Phys. Chem. Chem. Phys. 17 (2015) 17007–17015, https://doi.org/10.1039/c5cp01708d.
[25] P. Anzenbacher, S. Marchal, J. Palacký, E. Anzenbacherová, T. Domaschke, R. Lange, T. Shimizu, K. Kitanishi, M. Stranava, M. Stiborová, M. Martinkova, Pressure effects reveal that changes in the redox states of the heme iron complexes in the sensor domains of two heme-based oxygen sensor proteins, EcDOS and YddV, have profound effects on their flexibility, FEBS J. 281 (2014) 5208–5219, https://doi.org/10.1111/febs.13060.
[26] M. Stranava, M. Martínková, M. Stiborová, P. Man, K. Kitanishi, L. Muchová, L. Vítek, V. Martínek, T. Shimizu, Introduction of water into the heme distal side by Leu65 mutations of an oxygen sensor, YddV, generates verdoheme and carbon monoxide, exerting the heme oxygenase reaction, J. Inorg. Biochem. 140 (2014) 29–38, https://doi.org/10.1016/j.jinorgbio.2014.06.010.
[27] Y. Sasakura, S. Hirata, S. Sugiyama, S. Suzuki, S. Taguchi, M. Watanabe, T. Matsui, I. Sagami, T. Shimizu, Characterization of a direct oxygen sensor heme protein from Escherichia coli. Effects of the heme redox states and mutations at the heme-binding site on catalysis and structure, J. Biol. Chem. 277 (2002) 23821–23827, https://doi.org/10.1074/jbc.M202738200.
[28] D.J. Murphy, Determination of accurate KI values for tight-binding enzyme inhibitors: an in silico study of experimental error and assay design, Anal. Biochem. 327 (2004) 61–67, https://doi.org/10.1016/j.ab.2003.12.018.
[29] V. Fojtikova, M. Stranava, M.H. Vos, U. Liebl, J. Hranicek, K. Kitanishi, T. Shimizu, M. Martinkova, Kinetic analysis of a globin-coupled histidine kinase, AfGcHK: effects of the heme iron complex, response regulator, and metal cations on autophosphorylation activity, Biochemistry 54 (2015) 5017–5029, https://doi.org/10.1021/acs.biochem.5b00517.
[30] A.L. Chang, J.R. Tuckerman, G. Gonzalez, R. Mayer, H. Weinhouse, G. Volman, D. Amikam, M. Benziman, M.A. Gilles-Gonzalez, Phosphodiesterase A1, a regulator of cellulose synthesis in Acetobacter xylinum, is a heme-based sensor, Biochemistry 40 (2001) 3420–3426, https://doi.org/10.1021/bi0100236.
[31] J. Roy, S. Sen Santara, M. Bose, S. Mukherjee, R. Saha, S. Adak, The ferrous-dioxy complex of Leishmania major globin coupled heme containing adenylate cyclase: the role of proximal histidine on its stability, Biochim. Biophys. Acta 1844 (2014) 615–622, https://doi.org/10.1016/j.bbapap.2014.01.004.
[32] M. Morikawa, K. Izui, M. Taguchi, H. Katsuki, Regulation of Escherichia coli phosphoenolpyruvate carboxylase by multiple effectors in vivo. Estimation of the activities in the cells grown on various compounds, J. Biochem. 87 (1980) 441–449.
[33] S. Taguchi, T. Matsui, J. Igarashi, Y. Sasakura, Y. Araki, O. Ito, S. Sugiyama, I. Sagami, T. Shimizu, Binding of oxygen and carbon monoxide to a heme-regulated phosphodiesterase from Escherichia coli. Kinetics and infrared spectra of the full-length wild-type enzyme, isolated PAS domain, and Met-95 mutants, J. Biol. Chem. 279 (2004) 3340–3347, https://doi.org/10.1074/jbc.M301013200.
[34] H. Takahashi, M. Sekimoto, M. Tanaka, A. Tanaka, J. Igarashi, T. Shimizu, Hydrogen sulfide stimulates the catalytic activity of a heme-regulated phosphodiesterase from Escherichia coli (Ec DOS), J. Inorg. Biochem. 109 (2012) 66–71, https://doi.org/10.1016/j.jinorgbio.2012.01.001.
[35] Y. Du, G. Liu, Y. Yan, D. Huang, W. Luo, M. Martinkova, P. Man, T. Shimizu, Conversion of a heme-based oxygen sensor to a heme oxygenase by hydrogen sulfide: effects of mutations in the heme distal side of a heme-based oxygen sensor phosphodiesterase (Ec DOS), Biometals 26 (2013) 839–852, https://doi.org/10.1007/s10534-013-9640-4.
[36] F. Yan, V. Fojtikova, P. Man, M. Stranava, M. Martínková, Y. Du, D. Huang, T. Shimizu, Catalytic enhancement of the heme-based oxygen-sensing phosphodiesterase EcDOS by hydrogen sulfide is caused by changes in heme coordination structure, Biometals 28 (2015) 637–652, https://doi.org/10.1007/s10534-015-9847-7.
[37] V. Fojtikova, M. Bartosova, P. Man, M. Stranava, T. Shimizu, M. Martinkova, Effects of hydrogen sulfide on the heme coordination structure and catalytic activity of the globin-coupled oxygen sensor AfGcHK, Biometals 29 (2016) 715–729, https://doi.org/10.1007/s10534-016-9947-z.